Out-of-plane testing of seismically retrofitted URM walls using posttensioning

Najif Ismail[1], Peter Laursen[2] and Jason M. Ingham[3]

1. Corresponding Author. PhD Student, Department of Civil and Environmental Engineering, University of Auckland, New Zealand. Email: nism009@aucklanduni.ac.nz

2. Assistant Professor, Department of Architectural Engineering, California Polytechnic State University, San Luis Obispo, USA. Email: plaursen@calpoly.edu

3. Associate Professor and Deputy Head of Research, Department of Civil and Environmental Engineering, University of Auckland, New Zealand. Email: j.ingham@auckland.ac.nz

Abstract

The out-of-plane flexural testing of two (02) full scale unreinforced masonry (URM) walls seismically retrofitted using post-tensioning is reported. The selected wall configuration was representative of a common out-of-plane URM wall, achieving a percentage new building standard (% NBS) of 57 when evaluated using the New Zealand Society for Earthquake Engineering (NZSEE) guidelines. The test walls imitated heritage New Zealand URM construction by using recycled clay brick masonry laid in common bond pattern, with one header course after every three stretcher courses, and ASTM type O mortar was used. A low level pre-compression was applied using a single mechanically restrained tendon inserted into a cavity at the centre of the walls. Threaded mild steel bar with a coupler system (with tensile yield strength of 500 MPa) and sheathed greased seven-wire strand (with tensile yield strength of 1300 MPa) were tensioned with an initial force of 50 kN and 100 kN respectively. Behaviour of the seismically retrofitted URM walls using posttensioning was compared to the response of a non-retrofitted URM wall, with the out-of-plane flexural strength of the posttensioned masonry walls observed to range from 2.9 to 7.1 times the strength of the non-retrofitted URM wall. Several aspects pertaining to seismic behaviour of posttensioned masonry walls including tendon stress variation, damage patterns, force-displacement behaviour, initial stiffness, and displacement capacity were investigated. Furthermore, the results for the retrofitted walls were compared with equations developed in previous studies, and it was inferred that current predictive techniques give conservative values of out-of-plane flexural strength for high level of pre-compression.

Keywords: Posttensioning, unbonded, out-of-plane, seismic, testing, earthquake, retrofit, masonry

1. INTRODUCTION

New Zealand unreinforced masonry (URM) building stock consists of mostly pre-1931 URM structures, with many of these buildings contributing to New Zealand's architectural heritage. The early British migrants who settled in New Zealand used URM extensively in building construction, but a decline in the popularity of URM buildings came about due to their poor performance in the 1931 Hawke's Bay earthquake (Dowrick 1998; Russell et al. 2007). Consequently, the use of URM in new construction was restricted by government regulations in 1965 (SANZ 1965). A recent study has revealed that the existing New Zealand URM building stock primarily has load bearing URM walls and flexible wooden diaphragms and that there is a wide variation in material properties (Russell et al. 2007).

New Zealand is a high seismic risk country and has several active faults. It is located at the boundary of the Australian Plate and the Pacific Plate, periodically having earthquakes with a magnitude of over 7.0 on the Richter's scale, and with a shallow focal depth of less than 30 km (GNS 2005). But most of New Zealand's URM buildings have insufficient capacity to endure these high seismic demands and a survey showed that a moderate intensity earthquake can damage many existing URM buildings (EQC 1995). Due to concerns of heritage preservation, demolition of these historic URM buildings is undesirable, which results in seismic retrofit being necessary. Therefore, the current New Zealand legislation, the Building Act 2004, requires the Territorial Authorities to have a policy regarding the seismic improvement of earthquake prone URM building structures (Department of Building & Housing 2004).

In the event of an earthquake, self weight creates an out-of-plane bending in the wall and due to their low tensile strength, URM walls are prone to fail (Green 1993; Rutherford and Chekene 1990). However, the behaviour of out-of-plane URM walls also depends on the presence of cross walls and diaphragm stiffness and in particular walls with height to thickness 'h/t' ratios higher than 14 are prone to out-of-plane flexural failure (Ewing et al. 1981). These out-of-plane unstable URM walls, with low overburden load, can be seismically retrofitted by posttensioning (Curtin 1982; Ganz 1990; Laursen and Ingham 2004; Laursen et al. 2006; Rosenboom and Kowalsky 2004; Wight and Ingham 2008; Wight et al. 2006; Wight et al. 2007), but current design procedures for the seismic retrofit of URM walls using posttensioning is overly conservative and merits further research attention (Bean Popehn et al. 2008). Performance of posttensioned URM walls depends upon initial posttensioning force, tendon type and spacing, restraint conditions and confinement. Posttensioning can either be bonded when tendons are fully restrained by grouting the cavity, or left unbonded by leaving cavities unfilled. Since unbonded posttensioning is reversible and does not impact the architectural fabric of the building, it is deemed to be a desirable retrofit solution for URM building structures having important heritage value (Goodwin 2008).

2. CONSTRUCTION DETAILS

2.1. WALL SPECIFICATIONS

Wall dimensions are specified in Table 1. The two posttensioned walls PTB-01 and PTS-02 have same configuration as that of non-retrofitted wall, C-01, which was tested in the Civil Test Hall at the University of Auckland, New Zealand (Derakhashan and Ingham 2009).

Table 1. Wall dimensions and properties

Wall	Effective height h_e (mm)	Length l_w (mm)	Thickness t (mm)	Wall self-weight N_w (kN)	Masonry strength f'_m (MPa)	Tendon type	Initial pre-stress		Bearing stress $f_m{}^a/f'_m$ (ratio)
							P (kN)	f_{ps} (MPa)	
C-01*	3900	1170	220	19	5.3	-	-	-	-
PTB-01	3900	1170	220	19	5.3	TR[b]	50	442	0.32
PTS-02	3900	1170	220	19	5.3	S[c]	100	789	0.56

[a] $f_m=(N_w+P)/(A_b)$ where A_b is the area of bearing plate
[b] Threaded mild steel bar (500 MPa)
[c] Sheathed, greased high strength seven-wire strand (1300 MPa)
*Tested in a companion study and reported in Derakhashan and Ingham (2009)

The selected wall configuration was representative of a common out-of-plane URM wall, achieving a percentage new building standard (% NBS) of 57 when evaluated using the New Zealand Society for Earthquake Engineering (NZSEE) guidelines. Recycled clay bricks, salvaged from an old URM building, and ASTM type O mortar were used to imitate existing New Zealand URM building stock. For posttensioning of the two URM walls, a threaded mild steel bar and a sheathed greased seven wire strand were tensioned with an initial applied force of 50 kN and 100 kN respectively, corresponding to masonry axial stresses of 0.2 MPa and 0.4 MPa. As maximum stresses develop at mid height (hinge zone) when slender URM walls are subjected to seismic excitations, a single prestressed tendon with bearing plating is adequate to produce the required stresses in hinge zones by distributing axial stress at an angle of 45^o in the wall. Therefore, both walls were prestressed using one posttensioned tendon (threaded bar and strand) inserted at the centre of wall and steel bearing plates were used to avoid localized masonry crushing. Figure 1 shows the end anchorage details used for both tendons.

2.2. WALL CONSTRUCTION

The walls were constructed using a common bond pattern, with one header course after every three stretcher courses, by an experienced brick layer under supervision. Recycled clay bricks, being 220 mm × 110 mm × 90 mm high, were laid with roughly 15 mm thick mortar courses. A flexible 50 mm conduit was used to leave a cavity in the walls during construction and bricks were accordingly chiselled to accommodate the conduit. As there was no bond between masonry and tendon, the conduit encased tendons behaved as if they were placed in a cored cavity. It was gathered from discussions with specialised local construction contractors that for seismic retrofit of URM buildings, current techniques are capable of drilling a core cavity up to four stories with a precision of ±10 mm.

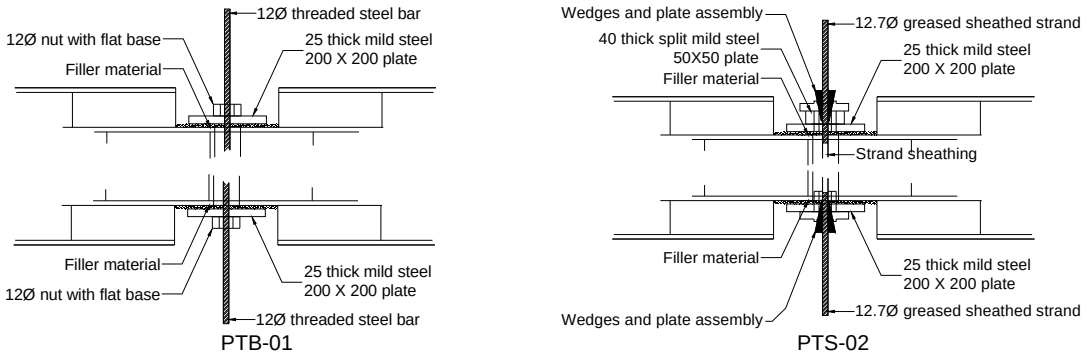

Figure 1. End anchorage details

Table 2. Material properties

	f'_m (MPa)	E_m (GPa)	C (MPa)	μ	f'_j (MPa)
Average	5.3	2.8	0.1	4.6	1.6

2.3. MATERIAL PROPERTIES

Average URM material properties were determined by material testing consistent with ASTM standards, typically in samples of three. Masonry compressive strength f'_m and masonry elastic modulus E_m were determined by testing three brick high prisms and mortar compressive strength f'_j was determined by testing three 50 mm by 50 mm cubes subjected to compression loading. Masonry cohesion C and coefficient of friction μ were investigated by bed joint shear testing of six three bricks high prisms with varying axial compression. Axial compression was applied to brick prisms using external posttensioned high strength bars. Table 2 shows the material properties and Figure 2 shows the graphical results of the tests.

Proof testing of each batch of tendons was perfomed by the New Zealand supplier and listed material properties were verified. For wall PTB-01 a threaded mild steel 12 mm diameter bar with a tensile yield strength f_{py1} of 500 MPa and an elastic modulus E_{s1} of 166 GPa was used with couplers (incl. flat base hexagonal nut and bearing plate at both ends of the tendon) as end anchorages. For wall PTS-02 a seven-wire prestressing strand with 12.7 mm diameter, greased and sheathed, with a tensile yield strength f_{py2} of 1300 MPa and elastic modulus E_{s2} of 180 GPa was used with end anchorage assembly as shown in Figure 1(b). In order to make posttensioning reverisble, to remove the strand (which is an architectural requirement for historic seismic retrofit), a 40 mm thick mild steel plate split in two halves was used, which can be removed to destress the strand.

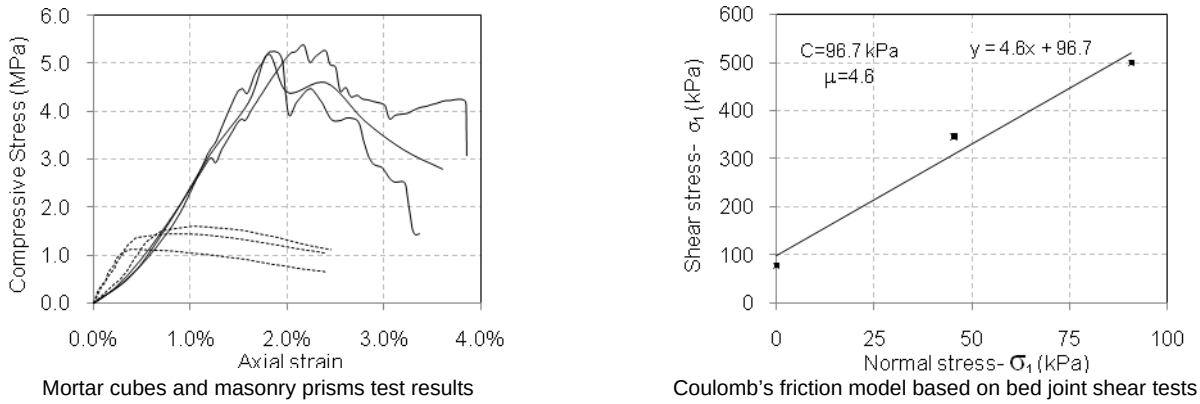

Mortar cubes and masonry prisms test results

Coulomb's friction model based on bed joint shear tests

Figure 2. Material test results

2.4. POSTTENSIONING

Test wall PTB-01 was posttensioned using a 10 kN hydraulic jack which was removed after tighting the nut to clasp the posttensioning bar. For test wall PTS-02 an electronic hydaulic jack was used to apply the initial posttensioning force and the taut strand was clapsed by wedge interlocking. Prestress levels detailed previously were ensured by applying required stress immediately before testing. Figure 3 shows photographs taken whilst the tendons were being tensioned.

(a) Posttensioning of PTB-01 (b) Posttensioning of PTS-02

Figure 3. Posttensioning of test walls

2.5. WALL BOUNDARY CONDITIONS

The wall configuration selected represents the worst case New Zealand URM wall, belonging to a single storey warehouse or a cathedral. It was presumed that the URM remains linearly elastic until cracking initiates and two segments started to rotate about the hinge formed at the mid height. Depending upon the construction of the building and wall location, the boundary conditions were selected and same rotational restraint were applied to the test wall which were consistent with earlier researchers hypothesis (Bean Popehn et al. 2008; Doherty et al. 2002; Lazzarini 2009). Generally, the URM walls are designed as simply supported one way slab, assuming that the end supports do not displace. Therefore a simple supported boundary conditions were used in the test setup and all other overburden loads were assumed to be a part of the pre-compression applied.

3. TESTING DETAILS

3.1. TEST SETUP

Testing of the posttensioned walls was conducted using the test rig shown in Figure 3, consisting of steel sections supporting a plywood backing frame, rigid steel reaction frame anchored to the concrete floor using sixteen 150 mm long M16 bolts, air bags capable of withstanding 15 kPa air pressure, air compressor, four S shape 2 volt load cells, frictionless plates, six steel clamps, steel connecting rods to connect load cells and the reaction frame, and a linear variable displacement transducer with stand. Air bags were used to apply a uniformly distributed pseudo-static load, emulating the lateral seismic load generated in the out-of-plane direction. The backing frame was placed over two greased steel plates with negligible friction, such that the backing frame self weight did not impair the test results. When air bags were inflated using the air compressor, the backing frame exerted force to load cells measuring the applied load on the test wall. The rigid reaction frame acted as a backing and also supported the top end of the wall, creating boundary conditions as if the posttensioned wall was connected to a diaphragm.

3.2. INSTRUMENTATION

One linear variable displacement transducer (LVDT) was located at wall mid-height to determine displacement and four S shape 2 volt load cells were used to determine the force

applied by air bags. One 300 kN load cell was installed at the top end of the posttensioning tendon to measure tendon stress.

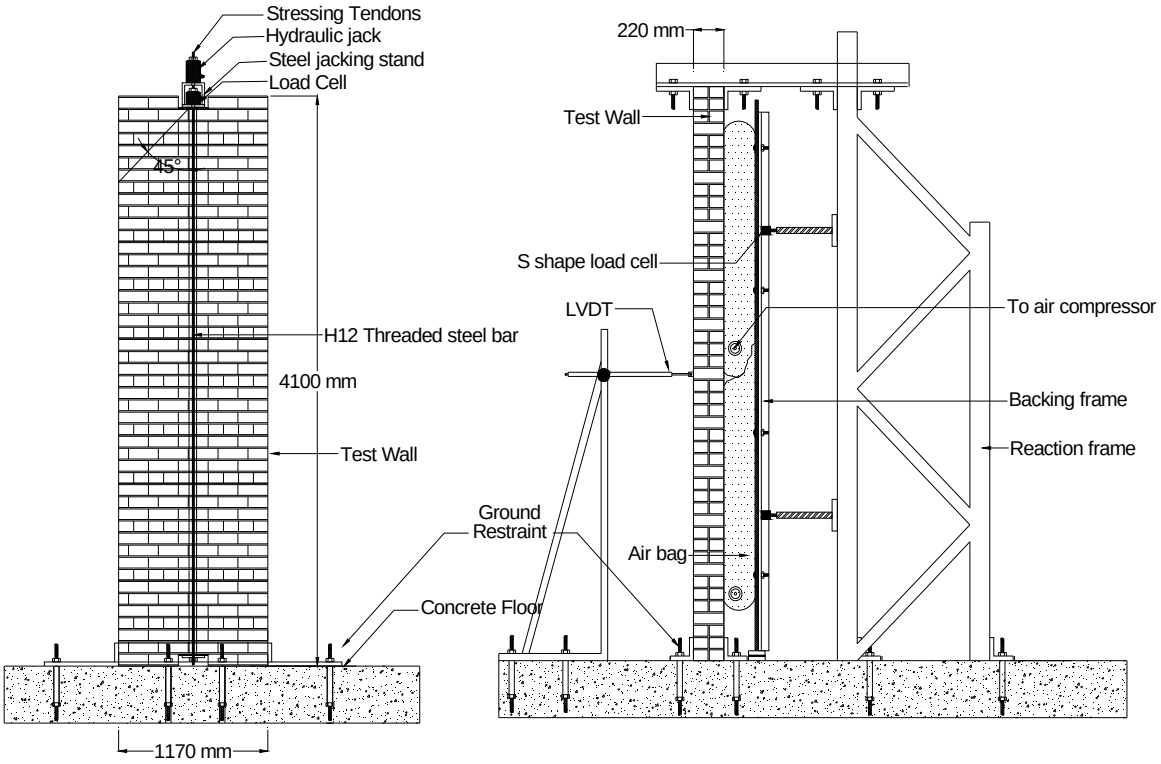

Figure 4. Test setup

4. TEST RESULTS

Test wall PTS-02 did not reach its ultimate flexural capacity before the test was stopped due to safety concerns and test wall PTB-01 was loaded up to its flexural capacity. A single large crack at or near mid-height and no flexurally distributed cracks were observed in both wall tests. However, localized brick punching was observed at some locations. Figure 5 shows photographs of the test setup and deflected test walls.

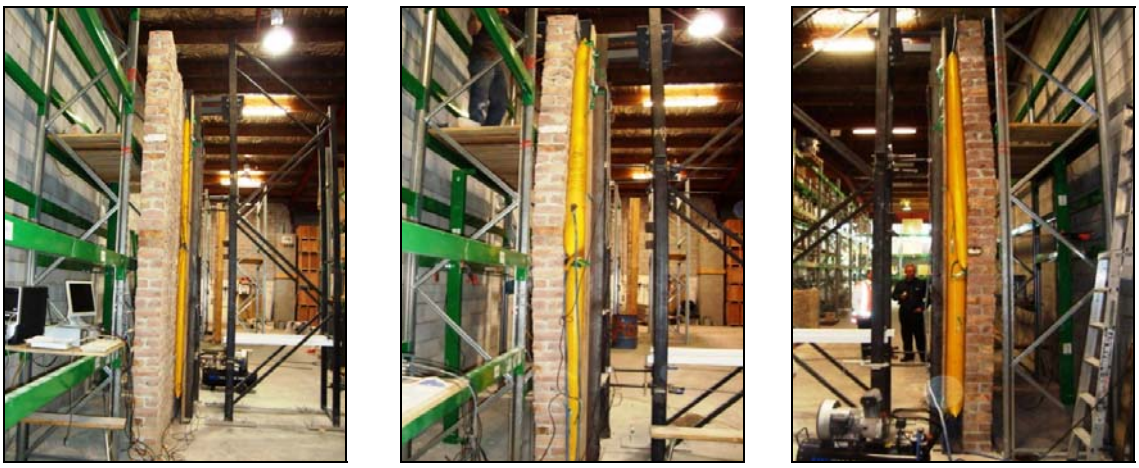

Test setup PTB-01 PTS-02

Figure 5. Photographs of testing

A gradual ductile failure mode was observed in wall PTS-02 with no residual deflection and strand stress did not exceed the specified elastic limit. In wall PTB-01 the threaded mild steel bar reached its elastic limit and yielded, causing strength degradation, but no visible residual deflections were observed. The test walls exhibited nearly non-linear elastic behaviour before bar yielding, which was attributed to the self centring behaviour of posttensioned masonry. The test walls' performance, when subjected to face loading, is summarized in Table 3 where V_u is the value of maximum total lateral force measured through load cells and M_u is the analogous moment applied at mid-height. Total load and moment, when first crack appeared, are denoted by V_c and M_c respectively. Flexural capacities at cracking and ultimate strength levels were predicted based on procedures advocated by Popehn et al. (2008) and were compared with experimental values.

$$M_c = \frac{I_n}{c}\left[f_r + \left(\frac{P_v + P_{sw} + A_{ps} f_{se}}{A_n} \right) \right] \quad (1)$$

$$M_n = \left(P_v + P_{sw} + A_{ps} f_{se}\right)\left[d_{eff} - \frac{\left(P_v + P_{sw} + A_{ps} f_{ps}\right)}{2\left(\lambda_n f_{bc} b\right)} \right] \quad (2)$$

The symbols used in Equations 1 and 2 are: M_c = applied moment at crack penetration; M_h = applied moment at hinge formation; M_n = moment capacity at nominal strength; I_n = net moment of inertia of the masonry; c = distance of extreme compression fibre to neutral axis; f_r = modulus of rupture; P_v = overburden vertical load producing axial compression on the masonry; P_{sw} = axial load due to self weight; A_{ps} = area of pre-stressing steel; f_{ps} = tensile stress in pre-stressing tendons at nominal strength; f_{se} = effective stress in pre-stressing tendons after all losses; A_n = net cross sectional area of the masonry; d_{eff} = distance of extreme compression fibre to centroid of tension reinforcement; f'_m = specified compressive strength of masonry; b = width of cross section; λ_h = parameter representing the fraction of maximum compressive stress at hinge formation; λ_n = parameter representing the fraction of maximum compressive stress at nominal strength. The ultimate displacement capacity was defined as $\gamma_u = d_u/h_{eff}$, where the ultimate displacement, d_u, is quantified by the measured displacement at hinge location when lateral strength has degraded below 80% of ultimate flexural capacity.

Table 3. Test results

Wall	Predicted values				Actual values				γ_u (%)	Comments
	V_c (kN)	V_n (kN)	M_c (kN.m)	M_n (kN.m)	V_c (kN)	V_u (kN)	M_c (kN.m)	M_u (kN.m)		
C-01*	-	-	-	-	-	2.2	2.1	2.1	3.0	Crack at mid-height, deflection controlled failure
PTB-01	4.2	6.6	2.1	3.2	4.6	6.3	2.2	3.1	0.8	Crack at mid-height, bar yielded
PTS-02	6.5	13.0	3.2	6.4	10.8	>15.3	5.2	>7.4	>1.9	Crack at mid-height, did not reach ultimate strength at 75 mm displacement

*Tested in a companion study and reported in Derakhashan et al. (2009)

4.1. FORCE-DISPLACEMENT RESPONSE

A positively sloped unloading branch was observed for wall PTS-02, which was attributable to the mechanics of the cross section details. When wall PTS-02 was subjected to large displacement, the prestressing tendon did not exceed its elastic limit and strand returned to its original position due to the restoring force, which was shown as the positive sloped unloading limb, following the same gradient as that of loading limb. Negatively sloped post peak behaviour of PTB-01, demonstrates the strength degradation due to mortar crushing at compression face and yielding of the mild steel bar. Negatively sloped post-peak branch has been observed in previous studies (Bean Popehn et al. 2008; Lacika and Drysdale 1995). Figure 6 (a and c) shows the force-displacement response for walls PTB-01 and PTS-02, with response of the non-retrofitted URM wall, C-01, depicted by a dotted line.

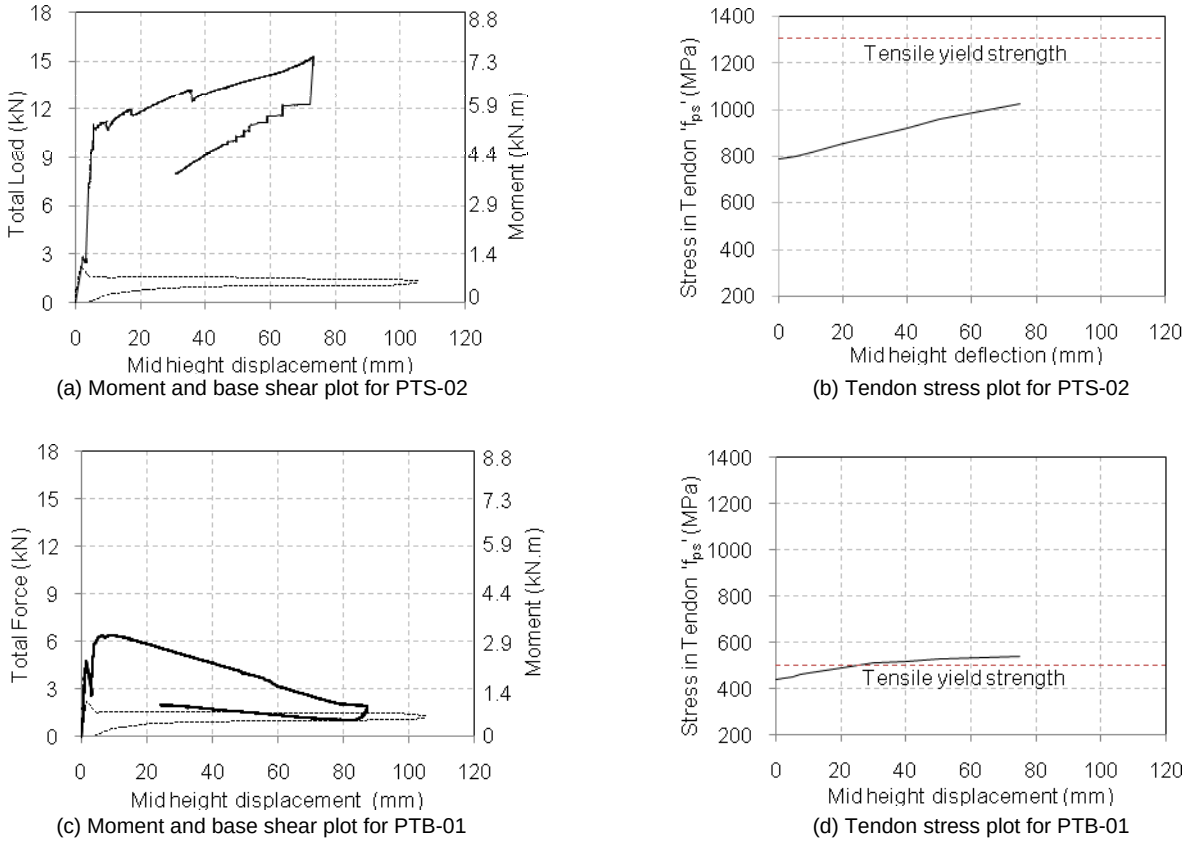

(a) Moment and base shear plot for PTS-02

(b) Tendon stress plot for PTS-02

(c) Moment and base shear plot for PTB-01

(d) Tendon stress plot for PTB-01

Figure 6. Wall response

Figure 7(a) shows the force-displacement plots for both posttensioned test walls. Test wall PTS-02 exhibited larger flexural capacity and less sensitivity to cracking than did wall PTB-01. Comparing results from the non-retrofitted wall and the posttensioned walls, it was determined that the nominal out-of-plane flexural strength of test walls PTB-01 and PTS-02 was respectively 2.9 times and 7.1 times the strength of the non-retrofitted URM wall. In order to correlate flexural capacities to corresponding ground excitations, results were transformed to ground accelerations using the ASCE 7-05 section 12 prescribed procedure. It was contemplated that the test walls belong to a URM building structure with potential historic value (i.e., I=1.25) which is resting over soft clay soil (i.e., C_{DS}=0.864 for site class E) and flexural capacities in terms of ground acceleration values were calculated using Equation 3, where W is the weight of the wall, C_s is the ground acceleration, F is the force at flexural failure in the test and h_w is the effective height.

$$C_s = \frac{2F}{Wh_{ip}} \qquad (3)$$

Figure 7(b) shows the ground acceleration values calculated by the procedure detailed in previous paragraph. It was inferred that the URM non-retrofitted wall was most likely to fail even under moderate intensity ground excitation of 0.11g, whereas, retrofitted walls PTB-01 and PTS-02 can sustain relatively high ground excitations of 0.32g and 0.78g respectively.

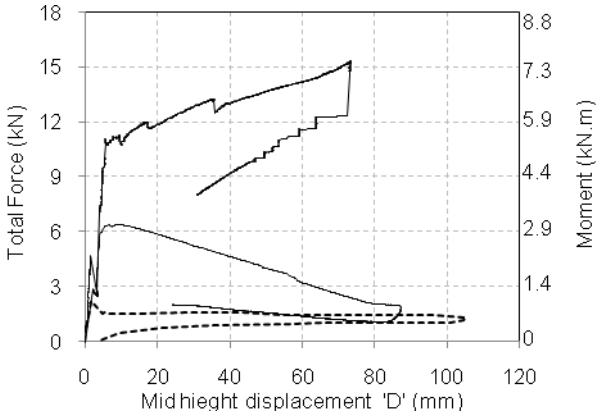

7 (a) Force displacement response

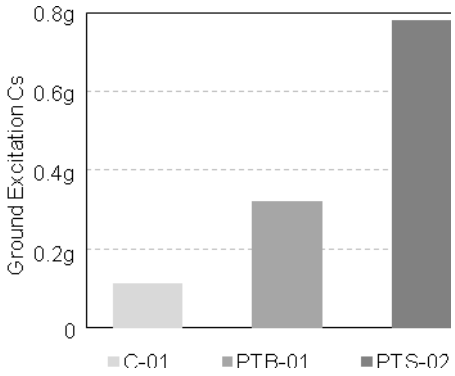

7 (b) Ground excitation corresponding to capacity

Figure 7. Comparison of wall response

4.2. TENDON STRESS

Figure 6 (b and d) shows the tendon stress histories plotted against the displacement at hinge location, which developed at or near wall mid-height in one way out-of-plane bending. It is noted that the dotted lines represent the tensile yield strength of tendons, which was 500 MPa for the threaded bar and 1300 MPa for the seven-wire strand. For wall PTB-01 the tendon stress started to increase at a faster rate after 25 mm displacement at the hinge location, corresponding to probable contact between the tendon and the face of the conduit, and reached its yield strength at nearly 28 mm mid-height displacement but did not reach its ultimate strength of 680 MPa. For wall PTS-02 strand stress increased linearly well within its elastic limit and no signs of strength degradation in the wall were observed. The increase in strand stress was nearly 30% of its initial stress.

4.3. INITIAL STIFFNESS

Initial stiffness is of considerable interest for dynamic modelling of a posttensioned URM wall when considering seismic behaviour of URM structures. The wall secant stiffness at or near cracking (corresponding to the first drop in force-displacement graph), K_c, varied for the test walls. However, the initial average stiffness, K_e, was quantified as the secant modulus between 0.05 and 0.3 of peak values and was nearly same for both walls. As initial average stiffness depends upon only wall dimensions and the elastic properties of masonry materials, this similarity in initial average stiffness fits well with theoretical knowledge.

4.4. FAILURE MODE AND DAMAGE PATTERNS

As discussed previously a horizontal crack opened at or near mid-height, and Figure 8 shows the photographs of the cracked wall sections.

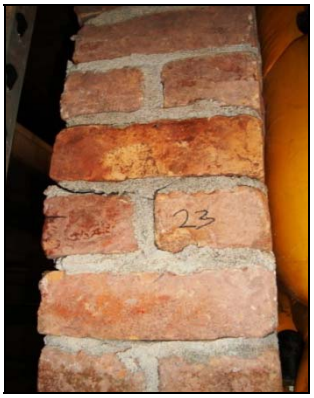

Wall PTB-01

Wall BTS-02

Figure 8. Photographs of damage pattern

5. CONCLUSIONS

Two URM walls retrofitted with varying level of posttensioning and different tendon types were tested for out-of-plane flexural strength, which were respectively 2.9 and 7.1 times the strength of a non-retrofitted wall, for initial pre-compression of 0.2 MPa and 0.4 MPa. It was therefore inferred that flexural capacity varied depending upon the initial posttensioning force and that the wall with high pre-compression showed less sensitivity to masonry cracking. For both retrofitted walls, only localized damage occurred, with a single crack at hinge location, which can be easily repaired following an earthquake.

In order to make retrofitted walls behave in a ductile fashion, the restoring force provided by the tendon is strongly desirable. Therefore, design must ensure that the increased tendon stress never reaches the yield strength of the tendon and an initial tendon stress of $0.55f_{pu}$ is recommended.

Self centring response of posttensioned tendons observed in the experiment advocates seismic retrofit by using posttensioning, for prime valued historic structures or where an immediate occupancy after an earthquake is desired.

It was also inferred that the equations previously developed, based on the basic principles of mechanics, were reasonably precise to predict the flexural capacity of the wall PTB-01, having a lower value of pre-compression, but the flexural strength of wall PTS-02, having a higher value of pre-compression, was much higher than the predictive values.

6. ACKNOWLEDGEMENTS

This research was conducted with financial support from Reid Construction Systems. The Higher Education Commission of Pakistan provided funding for doctoral studies of the first author. The authors are gratified to Derek Lawley, Yi Wei Lin, Hossein Derakhshan, Terry Seagrave, Garath Williams and Tek Goon Ang for help with the experimental setup. Thanks are also extended to Win Clark for their valued feedback.

7. REFERENCES

Bean Popehn, J. R., Schultz, A. E., Lu, M., Stolarski, H. K., and Ojard, N. J. (2008). "Influence of transverse loading on the stability of slender unreinforced masonry walls." *Engineering Structures*, 30(10), 2830-2839.

Curtin, W. G. (1982). *Development, application and potential of reinforced and prestressed masonry*, London.

Department of Building & Housing, N. (2004). "The Building Act." N. Department of Building & Housing, ed., Victoria University Book Centre, Wellington, New Zealand.

Derakhashan, H., and Ingham, J. M. (2009). "Out-of-plane assessment of unreinforced masonry walls." Univeristy of Auckland, Auckland.

Doherty, K., Griffith, M. C., Lam, N., and Wilson, J. (2002). "Displacement-based Seismic Analysis for the Out-of-plane Bending of Unreinforced Masonry Walls." *Earthquake Engineering and Structural Dynamics*, 31, 833-850.

Dowrick, D. J. (1998). "Damage and intensities in the magnitude 7.8 1931 Hawke's Bay, New Zealand, earthquake." *Bulletin of the New Zealand National Society for Earthquake Engineering*, 31(3), 139-162.

EQC. "The scenario: the great Wellington quake of 1995." *Wellington after the 'quake: the challenge of rebuilding cities, Earthquake Commission and Centre for Advanced Engineering*, Wellington, New Zealand, 3-5.

Ewing, Robert, D., and Kariotis, J. C. (1981). "Methodolgy for mitigation of seismic hazards in existing unreinforced masonry buildings: Wall testing, out-of-plane, a joint venture of Agbabian Associates, S.B. Barnes and Associates and Kariotis and Associates (ABK)." *04*, El Segundo, CA.

Ganz, H. R. (1990). "Posttensioned masonry structures." VSL International Ltd., Berne, Switzerland.

GNS. (2005). "The Active Earth." GNS Science Limited.

Goodwin, C. (2008). "Architectural and historic considerations for the seismic retrofit of URM buildings," Masters Thesis, Univeristy of Auckland, Auckland, New Zealand.

Green, M. (1993). "Code provisions for unreinforced masonry bearing wall buildings in California." Symposium on Structural Engineering in Hazard Mitigation, American Society of Civil Engineers, Irvine, CA, United States.

Lacika, E. M., and Drysdale, R. G. "Experimental investigation of selender prestressed brick walls." *7th Canadian Masonry Symposium*, Hamilton Ontario, Canada, 724-735.

Laursen, P. T., and Ingham, J. M. (2004). "Structural testing of large-scale posttensioned concrete masonry walls." *Journal of Structural Engineering*, 130(10), 1497-1505.

Laursen, P. T., Wight, G. D., and Ingham, J. M. (2006). "Assessing creep and shrinkage losses in post-tensioned concrete masonry." *ACI Materials Journal*, 103(6), 427-435.

Lazzarini, D. L. (2009). "Seismic Performance of Unreinforced Masonry Walls Retrofitted with Post-Tensioning Tendons," Masters Thesis, California Polytechnic State University, San Luis Obispo, California.

Rosenboom, O. A., and Kowalsky, M. J. (2004). "Reversed in-plane cyclic behavior of posttensioned clay brick masonry walls." *Journal of Structural Engineering*, 130(5), 787-798.

Russell, A. P., Mahmood, H., and Ingham, J. M. "Assessment of the material properties of New Zealand's unreinforced masonry building stock." *The Third International Conference on Structural Engineering, Mechanics and Computation*, Cape Town, South Africa.

Rutherford and Chekene. (1990). "Seismic retrofitting alternatives for San Francisco's unreinforced masonry buildings: Estimates of construction cost and seismic damage for the San Farncisco department of city planning." Rutherford and Chekene Consulting Engineer, San Francisco CA.

SANZ. (1965). *NZS 1900: 1965; Model building bylaw*, Standards New Zealand, Wellington, New Zealand.

Wight, G. D., and Ingham, J. M. (2008). "Tendon stress in unbonded posttensioned masonry walls at nominal in-plane strength." *Journal of Structural Engineering*, 134(6), 938-946.
Wight, G. D., Ingham, J. M., and Kowalsky, M. J. (2006). "Shaketable testing of rectangular post-tensioned concrete masonry walls." *ACI Structural Journal*, 103(4), 587-595.
Wight, G. D., Ingham, J. M., and Wilton, A. R. (2007). "Innovative seismic design of a post-tensioned concrete masonry house." *Canadian Journal of Civil Engineering*, 34(11), 1393-1402.